



# Biosorption of Methylene Blue Dye onto Three Different Marine Macroalgae: Effects of Different Parameters on Isotherm, Kinetic and Thermodynamic

Ehsan Daneshvar<sup>1</sup> · Arya Vazirzadeh<sup>1</sup> · Amit Bhatnagar<sup>2</sup>

Received: 22 April 2019 / Accepted: 22 August 2019 / Published online: 13 September 2019  
© Shiraz University 2019

## Abstract

In the present study, the removal of a cationic dye, methylene blue (MB) with brown (*Nizamuddinina zanardinii*), red (*Gracilaria parvispora*) and green (*Ulva fasciata*) macroalgae was studied. The effects of different parameters such as initial solution pH, initial dye concentration, biomass dosage and contact time were investigated on the biosorption of MB by algae. Biosorption isotherm was modeled using the Langmuir, Freundlich and Temkin models. The highest MB dye removal efficiency onto algae was observed in the range of 5–11. Increasing biosorbent dosage from 80 to 240 mg/L, significantly increased the removal efficiency of MB dye; however, increasing the biosorbent dosage above 240 mg/L up to 400 mg/L did not significantly increase the dye removal efficiency. The biosorption of MB dye onto macroalgae reached equilibrium after about 90 min. Based on the Langmuir model, the uptake of MB by brown, red and green algae was determined as 863.4, 83.08 and 1514 mg/g, respectively. The biosorption kinetic data were successfully described with pseudo-second-order model for three biosorbents. FT-IR spectrum analysis suggested amido or hydroxyl, C=C and C–H groups present on algae surface could take part in MB dye biosorption.

**Keywords** Biosorption · Textile dyes · Macroalgae · Isotherm · Thermodynamics

## 1 Introduction

Due to the generation of huge volumes of urban and industrial wastewater in both developed and developing countries, and also due to the associated risk of dumping toxic effluents into rivers, lakes and/or sea, it is important to treat wastewaters to reduce the contamination of global aquatic environment (Daneshvar et al. 2017a).

Many inorganic and organic pollutants, e.g., heavy metals, nitrate, phosphate and dyes, are generally present in industrial effluents. Among them, dyeing effluents from textile, leather, cosmetics, paper, plastics and other related industries cause serious environmental problems (Kousha

et al. 2015). Very low concentrations of dyes make the water undesirable and highly sensible and have bad aesthetic effects. These hazardous pollutants are toxic, carcinogenic and mutagenic for human and other organisms and increase the chemical oxygen demand (COD) in aquatic environments (Lee et al. 1999).

According to the general structure, the textile dyes are classified as anionic (direct, acid and reactive), nonionic (disperse) and cationic (basic) dyes (Mishra and Tripathy 1993). Cationic dyes consist of amino groups, or alkyl amino groups, as their auxochromes. Among basic dyes, methylene blue (MB) is a heterocyclic aromatic compound that is used for dyeing leather, printing calico, cotton and tannin, and for medicinal purposes in its purified zinc-free form (Gupta et al. 2004). In aquaculture, it is also used to prevent fungal and bacterial infection of newly laid fish eggs. This easy water-soluble dye can cause eye/skin irritation, vomiting, shock, increasing heart rate and systemic effects including cyanosis and blood changes (Papic et al. 2000). Thus, it is necessary to remove synthetic dyes

✉ Arya Vazirzadeh  
vazirzadeh@shirazu.ac.ir

<sup>1</sup> Department of Natural Resources and Environmental Engineering, School of Agriculture, Shiraz University, Shiraz 71441-65186, Iran

<sup>2</sup> Department of Environmental Science, University of Eastern Finland, P.O. Box 1627, 70211 Kuopio, Finland

including MB before they enter downstream bodies of water.

The complex structures and synthetic origin of dyes make them very difficult to decompose and degrade. Therefore, developing efficient methods for the treatment of dye effluents is a crucial challenge.

In general, different chemical, physical and biological methods have been applied for wastewater treatment (Deniz 2019). Well-known treatment methods include adsorption, coagulation/flocculation, advanced oxidation processes (AOPs), membrane filtration, irradiation, photocatalytic degradation, anaerobic/aerobic treatment, bioaccumulation and (bio)adsorption/biosorption (Deniz 2019; Zhang et al. 2019). However, all these methods have their own advantages and disadvantages such as high operational and maintenance cost, toxic by-products or sludge generation and fouling (Azin and Moghimi 2018).

Among the various dyes removal techniques, biosorption using low-cost materials has attracted researcher's attention in recent years. It can be defined as sequestering of organic or inorganic compounds by dead biomass or their derivatives of bacteria, fungi, yeasts, algae, seaweeds and even industrial or agricultural wastes (Khataee and Dehghan 2011). In recent years, many studies have been carried out with macroalgae for the removal of aquatic pollutants especially heavy metals (He and Chen 2014).

The literature shows that the marine algae can be used as a renewable source for treating effluents containing heavy metals, dyes and other contaminants. Macroalgae usage as biosorbents is associated with their high biosorption capacity, and their availability in large quantities in many regions of the world (Daneshvar et al. 2012b). Their cell walls that include a fibrous skeleton and an amorphous embedding matrix have the main effect on their biosorption capacity. The main component of the fibrous skeleton is the cellulose that it can be constituted by other hemicelluloses.

The presence of different polysaccharides in marine macroalgae cell walls is the reason why diverse groups of brown, red and green algae have different biosorption ability. These algae have different types and amounts of chemical functional groups such as carboxyl, amine, imidazole, phosphate, sulfate, sulfhydryl and hydroxyl in their cell walls. The difference between algae sorption capacity could be referred to their cell wall components, topography and cationic/anionic sites. As an example, more anionic sites could show the high affinity for positively charged basic dyes, but lower affinity for anionic dyes.

Here, we have investigated the biosorption capacity of three macroalgae, viz. brown (*Nizamuddinina zanardinii*), red (*Gracilaria parvispora*) and green (*Ulva fasciata*) toward methylene blue dye removal from aqueous solution. For this purpose, the main factors that influence the removal of dye onto marine algae were investigated to

understand their impact on the process. The biosorption experiments included isotherms, kinetics and thermodynamic studies. To obtain the information on the possible interactions between the functional groups of biomasses (algae) and MB, and comparison between algae surface structure, all biosorbents were characterized by Fourier transform infrared spectroscopy (FT-IR), and scanning electron microscopy (SEM).

## 2 Materials and Methods

### 2.1 Characterization of Biosorbents

The marine macroalgae samples before and after MB biosorption were characterized using FT-IR and SEM analysis. For FT-IR sampling, a sample of brown, red and green algae before and after MB biosorption were dried and coated with KBr to form pellets and analyzed using PerkinElmer FT-IR within the range of 400–4000  $1/\text{cm}$  by a spectrometer, model Spectrum RXI. The algae morphology after gold coating was studied using scanning electron microscope (SEM, Tescan, Czech Republic).

### 2.2 Preparation of Biosorbents

Three marine macroalgae, viz. *N. zanardinii*, *G. parvispora* and *U. fasciata*, were collected from the Oman Sea coast of Chabahar, Iran. Before use, all macroalgae were washed several times with tap water to remove extraneous materials and salts. The washed biomasses were sun-dried for 48 h and dried in an oven at 60 °C for 24 h. Then, these were cut and sieved into segments of 106–250  $\mu\text{m}$  and were used for the experiments.

### 2.3 Preparation of MB Solution

Methylene blue ( $\text{C}_{16}\text{H}_{18}\text{N}_3\text{SCl}$ ; MW: 319.85 g/mol,  $\lambda_{\text{max}} = 664 \text{ nm}$ ) was provided from Alvan Sabet, Iran, and stock solution with 500 mg/L concentration was prepared by dissolving a weighed amount of the dye in distilled water. Other MB solutions were prepared by diluting MB stock to obtain different concentrations of 2.5–240 mg/L.

### 2.4 Biosorption Studies

Biosorption experiments were conducted using 100 mL capped Erlenmeyer flasks containing 50 mL of MB solution. The mixture of adsorbate and adsorbent was agitated in the temperature-controlled incubator shaker (130 rpm at 28 °C) (Jal Tajhiz, JTSL40), until the equilibrium was reached. The following parameters were used in the series of biosorption experiments: the effect of initial solution

pH: 2, 3.5, 5, 6.5, 8, 9.5 and 11 (algae dosage: 240 mg/L, MB concentration: 10 mg/L, time: 90 min), biomass loading: 80, 160, 240, 320 and 400 mg/L (initial solution pH: 6.5, MB concentration: 10 mg/L, time: 90 min), initial MB concentration: 2.5, 5, 10, 15, 20, 40, 80, 160 and 240 mg/L (initial solution pH: 6.5, algae dosage: 240 mg/L, time: 90 min), contact time: 0–180 min (initial solution pH: 6.5, algae dosage: 240 mg/L, MB concentration: 10 mg/L) and temperature (initial solution pH: 6.5, algae dosage: 240 mg/L, MB concentration: 10 mg/L, time: 90 min).

After equilibrium, the solution was centrifuged and subsequently was analyzed for residual dye concentration. The concentration of the unadsorbed MB was analyzed with a UV/Vis spectrophotometer (UVVIS-Spectrophotometer, SP-3000 IUS). The absorbance of color was recorded at 664 nm where the maximum absorption peak exists.

The following equations were used to calculate the amount of MB adsorbed onto marine macroalgae.

$$R\% = C_i - C_f / C_i \times 100 \quad (1)$$

$$q_e = V(C_i - C_f) / m \quad (2)$$

where  $R$  is MB removal efficiency (%),  $q_e$  (mg/g) is the amount of dye biosorbed per gram of biosorbent at equilibrium,  $C_i$  and  $C_f$  are the initial and equilibrium MB concentration in the solution (mg/L), respectively,  $V$  is the MB solution volume (L), and  $m$  is the algae mass (g).

## 2.5 Biosorption Isotherms

Biosorption isotherms were carried out in 100 mL Erlenmeyer flasks containing 50 mL dye solution. The known amount of biosorbents was suspended in MB solution, and mixture was agitated on the temperature-controlled incubator shaker (130 rpm and 28 °C), until the equilibrium was reached. The most common isotherm models, namely the Temkin, Freundlich and Langmuir, were applied to determine the relationship between adsorbed MB dye on the algal biomasses and unadsorbed MB in solution.

## 2.6 Biosorption Kinetics

The biosorption kinetics were studied by varying the contact time between 0 and 180 min in 500 mL conical flasks containing 200 mL of the dye solution (10 mg/L) and biosorbent dose of 240 mg/L (48 mg of the algae biomass/200 mL MB). At predetermined time intervals, 5 mL samples were withdrawn and measured for the residual MB concentration. The kinetic data were analyzed using pseudo-first-order, pseudo-second-order and intra-particle diffusion models.

## 2.7 Biosorption Thermodynamics

Biosorption of MB dye onto three marine algae was investigated at three different temperatures (285, 293 and 301 K) in an incubator shaker under pre-optimized conditions, specifically 240 mg/L algae mass, 10 mg/L initial MB concentration, pH 6.5 and 130 rpm. The main thermodynamic parameters such as changes in the Gibbs free energy ( $\Delta G$ ), enthalpy ( $\Delta H$ ) and entropy ( $\Delta S$ ) were used to assess the spontaneity and endo/exothermic nature of the biosorption process.

## 3 Results and Discussion

### 3.1 FT-IR Spectra

To understand any possible interaction between the functional groups on the surface of the marine macroalgae and MB dye, dried powder of three algae was examined using FT-IR spectroscopy before and after dye biosorption (Fig. 1a–c). The broad absorption band in the spectrum of natural biomass at 3398.77 (brown alga), 3418.65 (red alga) and 3427.49 1/cm (green alga) is likely to be due to the overlap of O–H and N–H stretching vibrations, indicating the presence of both surface hydroxyl stretching of carboxylic groups and also stretching of amido groups. The peaks observed at 2928.63, 2926.77 and 2927.55 1/cm were assigned to the C–H stretching vibrations of the aliphatic groups. The other strong bands around 1600 1/cm were attributed to  $-C = C$  stretching. The broad peaks at 1424.63, 1466.35 and 1421.01 1/cm represented the presence of C–H bend. The bands at 1230–1270 1/cm were assigned to the aromatic ethers, aryl-O stretching. The band observed at 1050–1150 1/cm could be assigned to C–H–C to the alkyl-substituted ether, C–O stretching. The bands at 600–620 1/cm are due to the disulfides (S–S stretch) (Coates 2000).

The FT-IR spectra of algae powder before dye biosorption show a number of peaks reflecting the complex nature of brown, red and green macroalgae surfaces. The intensity of the bands varied at different regions after interaction with MB dye. From the FT-IR spectra analysis of raw and MB-loaded biomass, it is clear that some functional groups are present on the macroalgae that have remarkable role in the dye biosorption process.

### 3.2 SEM Characterization

The SEM analysis is another useful tool for characterizing the surface morphology of the biosorbents. The morphology of dried marine algae powders before and after MB

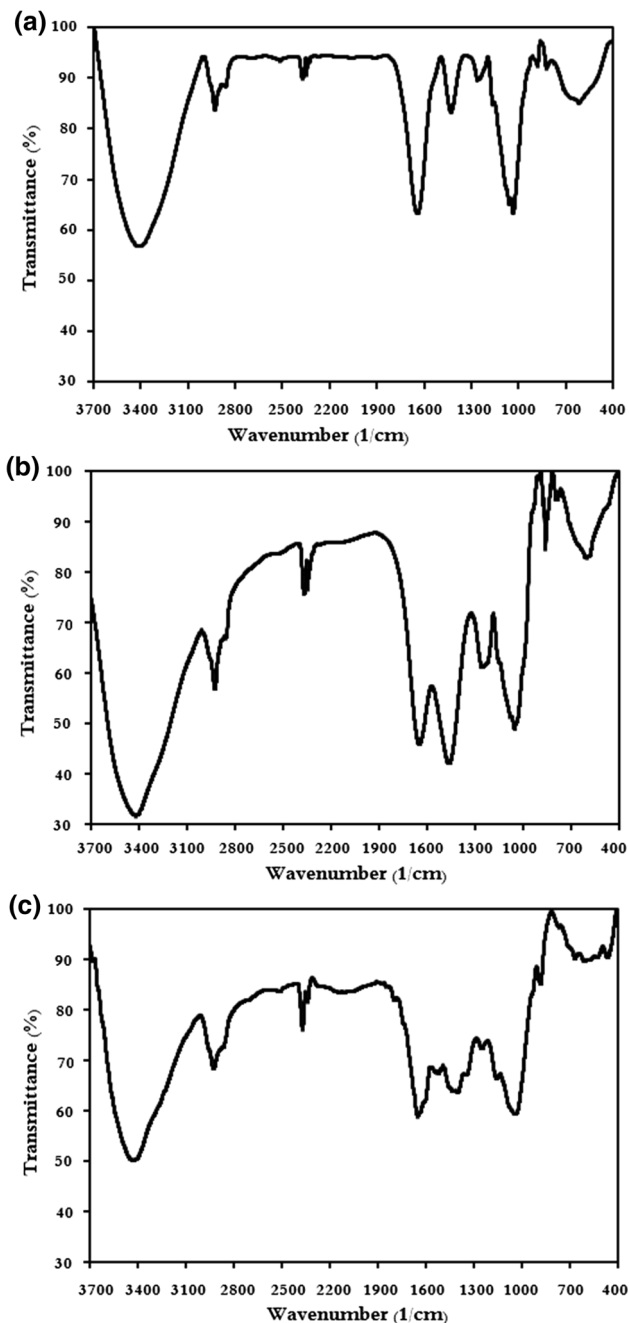


**Fig. 1** FT-IR spectra of brown, red and green algae before and after MB biosorption [brown alga (a), red alga (b), green alga (c)]

biosorption test is measured by SEM (Fig. 2a–f). As can be seen, there is a clear difference between brown, red and green marine macroalgae. There are numerous granule shapes on the brown alga surface (Fig. 2a). According to the surface to volume ratio, large areas for MB biosorption create by this granular surface. Also a large volume of pores are made by the aggregation of these tiny particles that increase biosorption capacity.

The SEM images revealed that red alga has a massy thick surface. The number of amorphous particles scattered on this surface. This morphology of red alga means thick external layers reduces the surface to volume ratio. As can be seen in Fig. 2c, there is not any effective cracks or cavities on this rough surface. The low biosorption capacity of red alga rather than brown and green algae could be related to its inefficient surface.

The unique characteristic of green alga that can be seen easily in the SEM image (Fig. 2e) is deep grooves and cavities beside together. On the other hand, the green alga surface is heterogeneous due to tiny bodies and bumps. The large surface area and grooved structure of green alga allow the molecules of MB dye to penetrate into the alga tissue and interact therein with the surface groups.

The SEM images revealed the difference between algae surface before and after MB biosorption clearly. The spaces between the particles on the surface of brown alga and the pores are filled out by the MB molecules. All of the granules are covered by MB dye and cannot be seen (Fig. 2b) after biosorption. As can be observed (Fig. 2d), the thick layers on the red alga surface changed to corrugated and wrinkled form after dye biosorption. Regarding to the green alga, all of the cracks and cavities on the alga surface are filled out after biosorption of MB dye. The irregular surface of green macroalga changed to smooth surface (Fig. 2f).

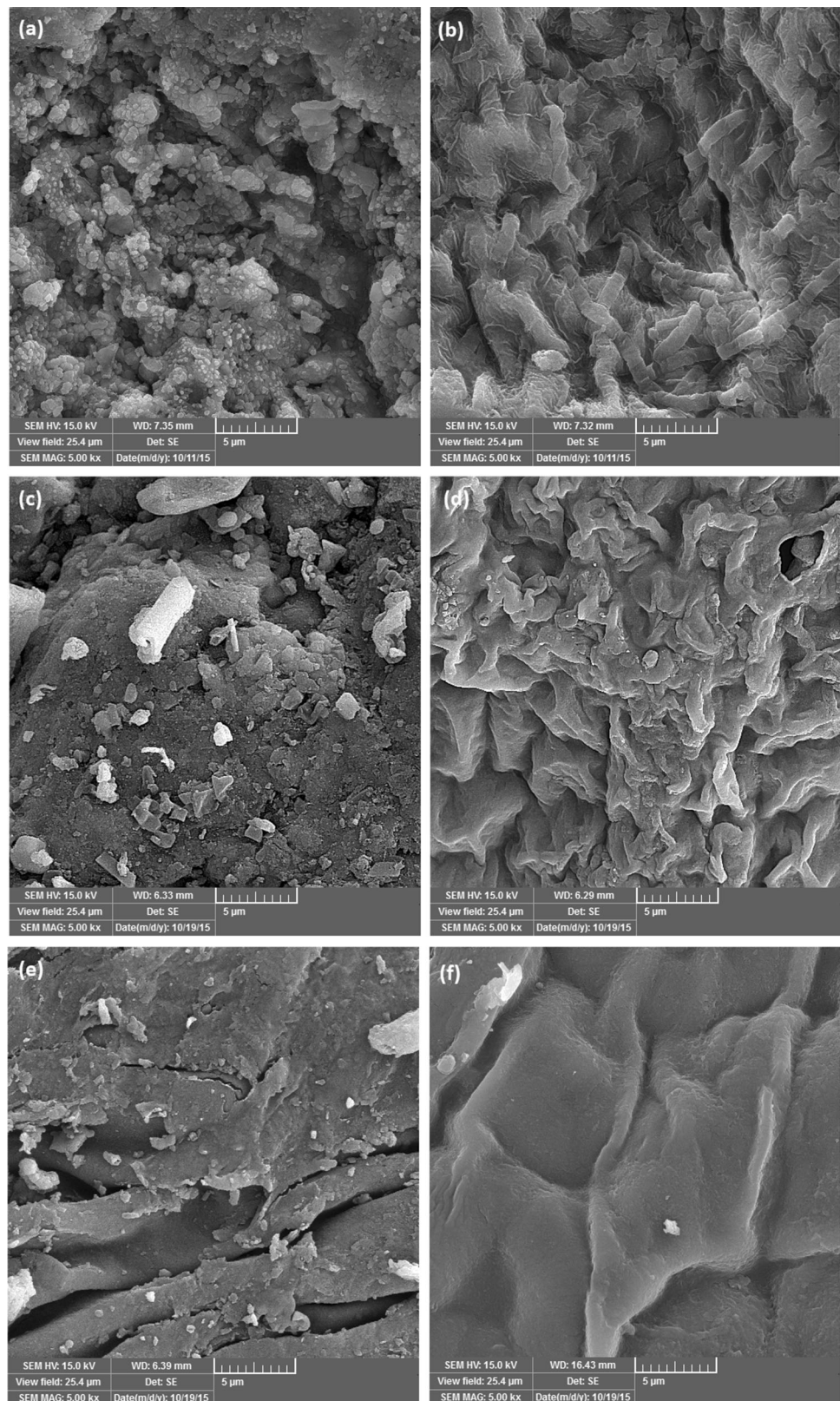
According to the SEM images, there are obvious differences between marine algae surface morphology. The different surface structure and functional groups of macroalgae cell wall have key roles on the dye biosorption capacity of macroalgae.

### 3.3 Effect of initial solution pH

Solution pH has a key role in dyes biosorption using algae, and it is the first factor that should be adjusted at the optimal pH zone. The pH of the solution may influence biosorption performance through different mechanisms including solute speciation (protonation/deprotonation of dyes and organic compounds, etc.), but also biosorbent surface properties (acid/base properties, for example) (Daneshvar et al. 2012a).

The biosorption experiments conducted in the initial pH range from 2 to 11 (Fig. 3a) shows that MB biosorption efficiency increased sharply as solution pH increased from 2 to 3.5 for brown and green algae and 2–5 for red alga. As can be seen from the curves, the increase of pH from 6.5 to 11 has no significant influence on removal efficiencies and maintained at a constant level. According to Fig. 3, the appropriate solution pH for MB biosorption onto algae is in the range of 5–11. The pH of point of zero charge ( $pH_{PZC}$ ) determines the pH at which the biosorbent surface has net

**Fig. 2** SEM images of brown, red and green Algae before and after MB biosorption [brown alga (**a**: before, **b**: after), red alga (**c**: before, **d**: after), green alga (**e**: before, **f**: after)]



electrical neutrality. In fact, at  $pH_{PZC}$ , there are the same amounts of anions and cations on the solid surface (Coelho

et al. 2014). In general, all algal species have an isoelectric point around pH 3–4 (Daneshvar et al. 2012b).

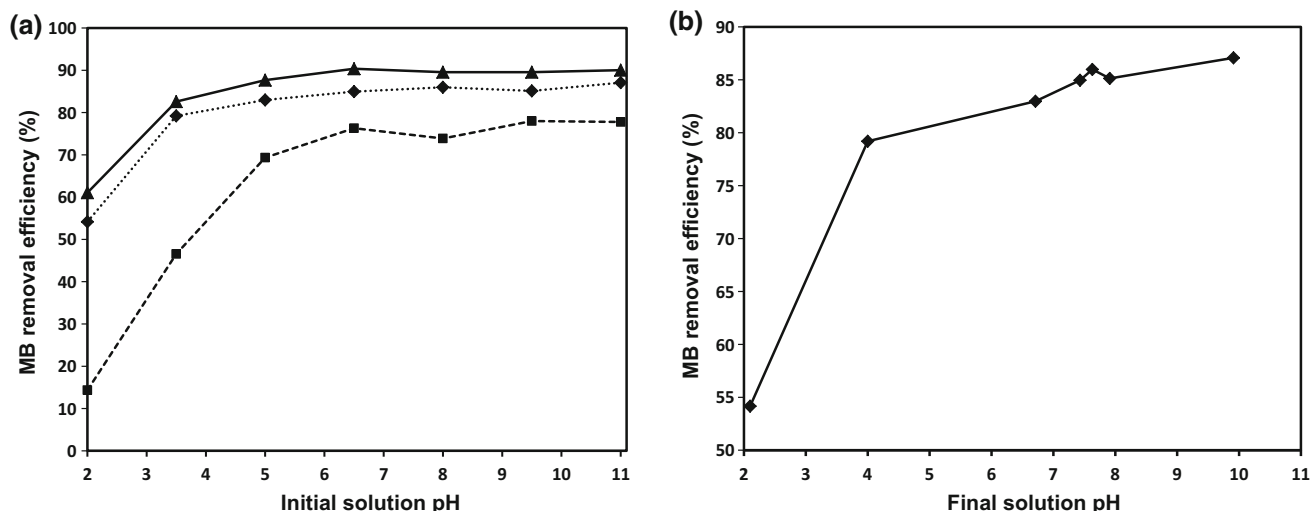


**Fig. 3** Effect of initial (a) and final (b) solution pH on MB removal efficiency [brown algae filled diamond, red algae filled square, green algae filled triangle]; algae dosage: 240 mg/L, MB concentration: 10 mg/L, time: 90 min

**Table 1** The initial solution pH changes during MB biosorption onto brown, red, and green macroalgae, after 90 min

Initial pH	Final pH			MB solution
	MB solution + algae			
	Brown	Red	Green	
2.02	2.1	2.09	2.09	2.1
3.56	4	3.82	4.19	3.56
5.06	6.71	6.92	7.01	5.72
6.54	7.43	7.48	7.42	7.05
8.08	7.63	7.58	7.72	7.5
9.5	7.91	7.88	7.88	8.59
11	9.91	9.88	9.87	9.98

At  $\text{pH} < \text{pH}_{\text{pzc}}$ , biosorbent surface is electropositive whereas at  $\text{pH} > \text{pH}_{\text{pzc}}$ , the surface is electronegative and favors the biosorption of cations. A large amount of  $\text{H}^+$  ions are present in acidic pH, which protonated the surface of algae biomasses and turn neutralized the negatively charged functional groups. Little biosorption in acidic zone of pH can be explained by the electrostatic repulsions of MB with the positively charged surface of the biomasses. At higher solution pH ( $\text{pH} > \text{pH}_{\text{pzc}}$ ), functional groups are deprotonated and electrostatic attraction can occur between the negatively charged functional groups and the positively charged cationic dye (Daneshvar et al. 2017b). Also as the pH increases, the competition between protons and basic dye for the same functional groups decreased and enhanced removal efficiency (Lima et al. 2019).

The final solution pH recorded for seven different initial pHs. Figure 3b illustrated the MB removal efficiency

against final solution pH. This graph and Table 1 show that there is a narrow final pH for the initial solution pH in the range 5–11. This effective zone of pH is higher than the  $\text{pH}_{\text{pzc}}$  (3–4), and the higher removal efficiency was observed here.

### 3.4 Effect of Algae Mass

Effect of biosorbent dosage is another important factor that influences the biosorption efficiency. At a specific dye concentration, it determines the availability of binding sites for removal of dye molecules. Optimization of this factor can help to improve the removal efficiency and prevents further expenses.

In this study, the effect of brown, red and green algae dose varying from 80 to 400 mg/L was investigated at optimized pH 6.5, initial MB concentration 10 mg/L at constant temperature. According to Fig. 4a, MB removal efficiency increased as algae dose increased from 80 to 240 mg/L. For the same concentration of MB dye, more binding sites are available at higher biomass dosage (Wang et al. 2019). However, increasing the biosorbent dosage above 240 mg/L did not significantly increase the dye removal efficiency. It expresses that there is an equal effective surface area for dye biosorption onto 240, 320 and 400 mg/L biomass dosage. In fact, after the efficient biomass dose, for a constant volume and specific concentration, dye removal efficiency was not affected by increasing algae dose.

Figure 4a depicts when the biomass dosages were increased from 80 to 400 mg/L, and the amount of the biosorbed MB decreased from 89 to 22 mg/g, 78 to 18 mg/g and 94 to 22 mg/g for brown, red and green algae, respectively. The higher amount of biosorbent aggregates

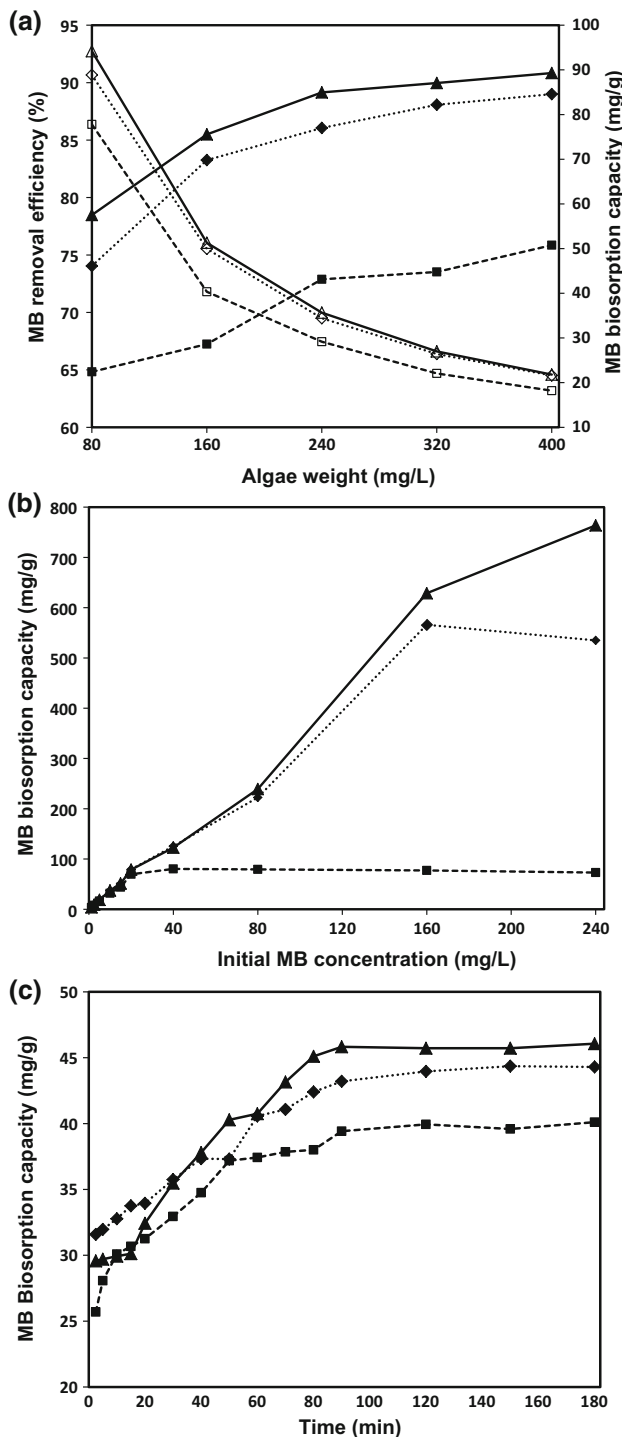


**Fig. 4** Effect of algae weight (a), initial MB concentration (b) and contact time (c) on MB removal efficiency and biosorption capacity [removal efficiency (%): brown alga filled diamond, red alga filled square, green alga filled triangle. Biosorption capacity (mg/g): brown alga open diamond, red alga open square, green alga open triangle]: initial solution pH: 6.5, MB concentration: 10 mg/L, time: 90 min

the algae particles and prevents to MB biosorption (Gupta and Rastogi 2008). On the other hand, the adsorbate/adsorbent interaction will be instead by adsorbent/adsorbent

at higher algae weight. Therefore, at lower biomass dosage, algae particles have more chance to cover by dye. So the amount of mg dye biosorption onto g biosorbent decreases as algae concentration increases. Our finding is in agreement with biosorption of Acid Blue 25, by aquatic plants (Kousha et al. 2014).

### 3.5 Effect of Initial MB Concentration

Optimized initial dye concentration is necessary to find maximum biosorption capacity ( $Q_{max}$ ) of the biosorbents. There is very little or no dye removal from aqueous solution after  $Q_{max}$ , for saturated biomass at higher concentration. On the other hand, unsaturated binding sites of biosorbent would be unused before  $Q_{max}$ , at lower concentration.

Effluents with high dye concentration could be treated by physical/chemical methods economically. Treatment of low concentration onto low-cost adsorbents is required in dye wastewater treatment. Here, the effect of initial MB concentration was investigated at different concentrations (1.25, 2.5, 5, 10, 15, 20, 40, 80, 160 and 240 mg/L). The results are presented in Fig. 4b. The graph illustrates that biosorption capacity of marine macroalgae significantly increased from 4.7 to 565.9, 3.7 to 80.33 and 3.9 to 763.7 mg/g for brown, red and green algae, respectively. It suggests that the higher MB concentration gradient provides an important driving force to overcome all mass transfer resistances of the dye molecules between the aqueous and solid phase (Doğan et al. 2006). When initial MB concentration increased from 160 to 240 mg/L, biosorption capacity decreased from 565.9 to 534.9 mg/g and 80.33 to 73.04 mg/g for brown and red algae, respectively. It shows that increasing the initial dye concentration increases dye biosorption until biosorbent saturation is achieved. In the case of green alga, linearly curve shows available unsaturated sites on surfaces of macroalga particles at this range of concentration. Similar results were also reported by other researchers for biosorption of three textile dyes by green algal *Spirogyra* sp. (Khataee et al. 2013).

### 3.6 Effect of Contact Time

The biosorption of MB onto different macroalgae was investigated as a function of contact time in order to determine the required time for maximum biosorption capacity. Brown, red and green alga (dose: 240 mg/L) were equilibrated with 200 mL of MB dye solution with an initial concentration of 10 mg/L at pH 6.5, while the contact time was changed from 2.5 to 180 min.

According to the depicted results in Fig. 4c, there are three fast, slow and stationary phases for MB biosorption process. A rapid biosorption rate occurred at the beginning

(phase 1), then dye molecules biosorbed gradually (phase 2) until the maximum biosorption capacity of biosorbents (phase 3) was reached. The initial rapid phase is due to the availability of large surface area and many vacant macropores for accumulation of MB, while the subsequent deceleration was due to the saturation of most of the available sites, and also due to the repulsive forces among adsorbed dye molecules and those present in the solution (Smaranda et al. 2009). In the third stage, the algae particles were saturated and biosorption process reached equilibrium. The same dye biosorption behavior was observed for three difference types of algae. It was concluded that a contact time of 90 min was sufficient for the biosorption to attain equilibrium.

### 3.7 Biosorption isotherms

Biosorption isotherms are the equilibrium relations between the amount of the solute on the solid phase (biosorbents) and in the liquid phase (dye solution) at a constant temperature. The value of dye sorption and desorption is equal for an equilibrium system; the value of retention/release of dye molecules at various concentrations could be describe by isotherm. In this experiment, MB concentration was varied (between 1.25 and 240 mg/L), while other process parameters were kept constant. The experimental data for the biosorption of MB on brown, red and green algae were fitted using three well-known isotherm models, viz., Langmuir (Langmuir 1918), Freundlich (Freundlich 1906) and Temkin (Temkin and Pyzhev 1940) which are explained at Table 2. The MATLAB software

**Table 2** Isotherm models, parameters and values for MB biosorption onto brown, red, and green macroalgae

Model/nonlinear form	Parameters (units)	Nomenclature	Value		
			Brown	Red	Green
Langmuir model $q_e = Q_0 b C_e / (1 + b C_e)$ (Equation 3)	$C_e$ (mg/L)	Equilibrium concentration	–	–	–
	$q_e$ (mg/g)	Amount of adsorbate in the adsorbent at equilibrium	–	–	–
	$Q_0$ (mg/g)	Maximum monolayer coverage capacities	863.4	83.08	1514
	$b$ (dm <sup>3</sup> /mg)	Langmuir isotherm constant	0.0321	0.3209	0.02263
	$R^2$	Correlation coefficient	0.9616	0.9191	0.9567
Freundlich model $q_e = K_F C_e^{1/n}$ (Equation 4)	$C_e$ (mg/L)	Equilibrium concentration	–	–	–
	$q_e$ (mg/g)	Amount of adsorbate in the adsorbent at equilibrium	–	–	–
	$K_F$ (mg/g) (dm <sup>3</sup> /g) <sup>n</sup>	Freundlich isotherm constant	47.62	30.12	48.02
	$n$	Biosorption intensity	1.641	4.911	1.374
	$R^2$	Correlation coefficient	0.9327	0.652	0.9326
Temkin model $q_e = RT/b_T (\ln A_T C_e)$ (Equation 5)	$C_e$ (mg/L)	Equilibrium concentration	–	–	–
	$q_e$ (mg/g)	Amount of adsorbate in the adsorbent at equilibrium	–	–	–
	$R$ (8.314 J/mol K)	Universal gas constant	8.314	–	8.314
	$T$ (K)	Temperature	301	–	301
	$b_T$ (g kJ/mg mol)	Temkin isotherm constant	128.2	–	110.4
	$A_T$ (L/g)	Temkin isotherm equilibrium binding constant	1.682	–	2.184
	$R^2$	Correlation coefficient	0.8327	–	0.8834



(Version 7.11.0 (R2010b)) was used to run nonlinear analysis of isotherms.

The Langmuir isotherm theory describes that monolayer biosorption takes place on the homogenous sites without any interaction between the biosorbed dye molecules on neighboring sites. This model assumes that there is equal energy for all sites. There are number of biosorption sites for a specific surface. According to the Langmuir model, when these sites are fully saturated, no further biosorption can take place. So the biosorbent has a finite capacity for the pollutant.

The Freundlich isotherm model is an empirical equation that corresponds a multilayer biosorption on to a heterogeneous surface with interaction between biosorbed dye molecules. Based on this model, the biosorption energy exponentially decreases on completion of the active sorption centers of a sorbent. The Freundlich constants  $K_F$  (biosorption capacity) and  $n$  (biosorption intensity) are empirical constants and affected by many environmental factors. The value of  $1/n$  smaller than unity or the value of  $n > 1$  represents favorable adsorption conditions.

The experimental data were also fitted to the Temkin isotherm, the third most popular isotherm model. This model is based on the assumption that the decline in the heat of sorption is linear rather than logarithmic (as implied in the Freundlich equation). The Temkin model considered some indirect adsorbate/adsorbent interactions that decrease the free energy of biosorption, as a function of the surface coverage. The Temkin model also assumes that sorption of dye molecules could be characterized by a uniform distribution of binding energies, up to some maximum value.

The parameters of the Langmuir ( $Q_0$  and  $b$ ) and Freundlich isotherm models ( $K_F$  and  $n$ ) determined by the intercepts and the slopes of the nonlinear plots of  $q_e$  versus  $C_e$  (Fig. 5). The obtained correlation coefficient of values can help to decide the suitable model. According to  $R^2$  presented in Table 2, the MB biosorption onto three different macroalgae follows the Langmuir model better than that the other ones. The biosorption isotherms revealed that the Langmuir biosorption capacities of marine algal biomasses were 863.4, 83.08 and 1514 mg/g for brown, red and green algae, respectively. The high biosorption capacity for MB indicates that marine algae investigated in this work have a considerable potential for cationic dye (MB) removal from aqueous solution.

### 3.8 Kinetic of Biosorption

High biosorption capacity and fast biosorption rate are considered as two significant characteristics of biosorbents. The experimental data for the biosorption of MB on brown, red and green algae were fitted using three kinetic models

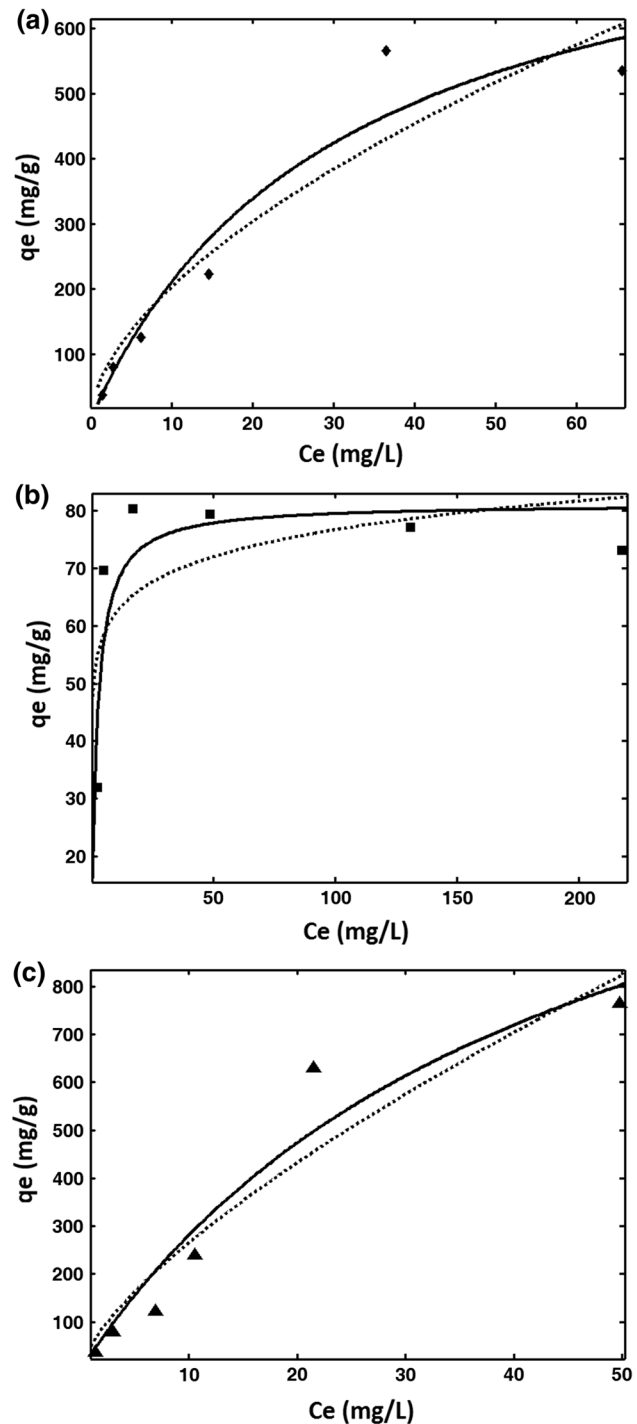


**Fig. 5** Langmuir and Freundlich isotherm models for the MB biosorption [brown alga filled diamond, red alga filled square, green alga filled diamond (solid line Langmuir, dotted line Freundlich)]: initial solution pH: 6.5, algae dosage: 240 mg/L, time: 90 min

namely, pseudo-first-order, pseudo-second-order and intra-particle diffusion model, which are explained as follows (Eqs. 6, 7 and 8):

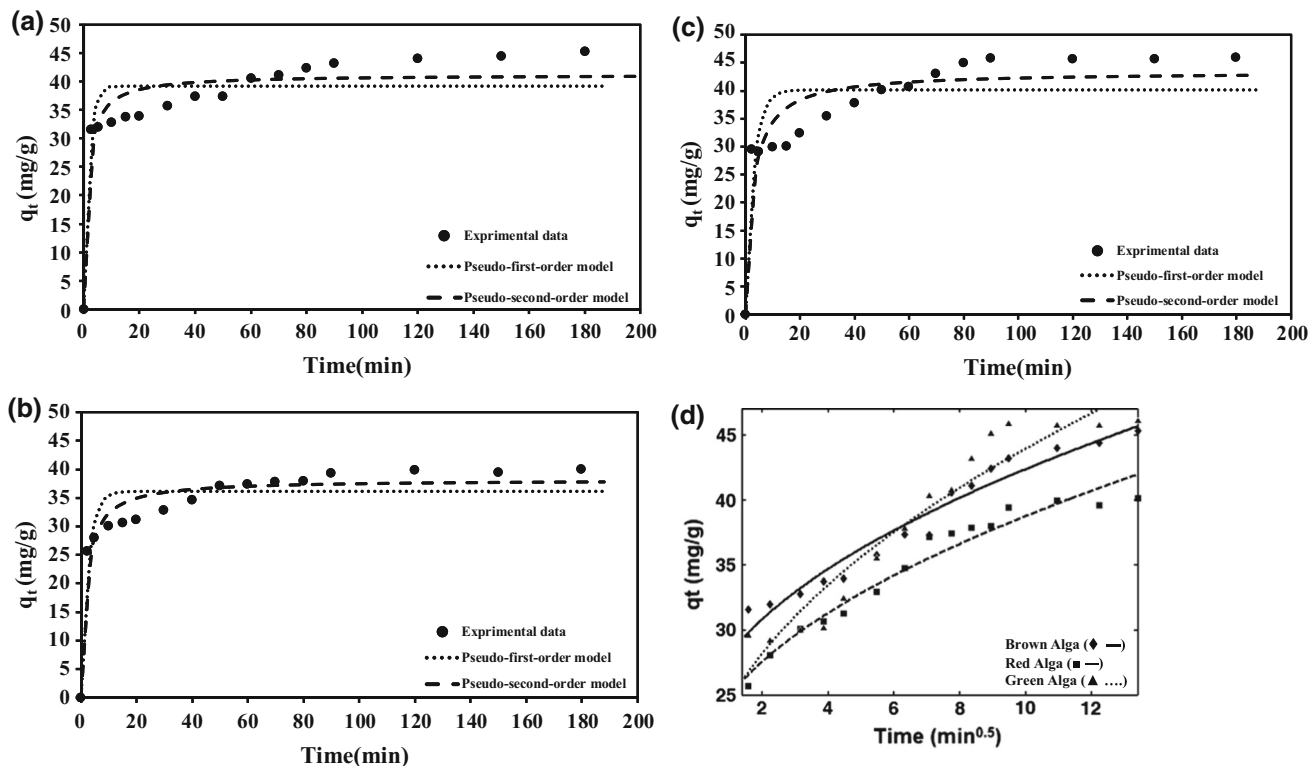


**Fig. 6** Pseudo-first-order, pseudo-second-order, and intra-particle diffusion (c) kinetic models for the MB biosorption [brown algae (filled diamond, solid line), red algae (filled square, dashed line), green

algae (filled triangle, dotted line)]; initial solution pH: 6.5, algae dosage: 240 mg/L, MB concentration: 10 mg/L

**Table 3** Kinetic parameters estimated by the pseudo-first-order, pseudo-second-order and intra-particle diffusion models (a) and thermodynamic parameters (b) for MB biosorption onto brown, red, and green macroalgae

Algae	Models								
	Pseudo-first-order			Pseudo-second-order			Intra-particle diffusion		
	$k_1$ (1/min)	$q_e$ (mg/g)	$R^2$	$k_2$ (g/mg min)	$q_e$ (mg/g)	$R^2$	$k_{id}$ (mg/g min <sup>0.5</sup> )	$c$ (mg/g)	$R^2$
Brown	0.528	39.23	0.921	0.018	41.16	0.954	6.601	21.48	0.951
Red	0.028	3.16	0.897	0.005	40.95	0.999	6.409	18.48	0.954
Green	0.379	36.18	0.939	0.014	38.19	0.974	9.017	15.42	0.922

$$q_t = q_e (1 - e^{-(k_1 t)}) \tag{6}$$

$$q_t = \frac{q_e^2 \times k_2 \times t}{1 + q_e \times k_2 \times t} \tag{7}$$

The parameters of pseudo-first-order and pseudo-second-order kinetic models are defined as follows:

$q_t$  (mg/g): the amount of MB adsorbed by algae at time  $t$ ,  $k_1$  (1/min): the constant of the pseudo-first-order model,  $t$  (min): time, and  $k_2$  (g/(mg min)): the rate constant of the pseudo-second-order model.

$$q_t = k_{id} t^{1/2} + C \tag{8}$$

where  $q_t$  (mg/g) is the amount of MB sorbed at time  $t$ ,  $C$  is the intercept (that corresponds to the lag phase when

resistance to film diffusion contributes to controlling uptake kinetics), and  $k_{id}$  (mg/gmin<sup>1/2</sup>) is the intra-particle diffusion rate constant.

Time (min) versus adsorption capacity (mg/L) of each microalga was plotted (Fig. 6a–c) and the calculated parameters values and their calculated parameters are shown in Table 3. The correlation coefficients of pseudo-first-order model were found to be 0.921, 0.897 and 0.939 for different brown, red and green macroalgae, respectively. It represented that the MB biosorption onto red and green algae were not well fitted by pseudo-first-order kinetic model. The pseudo-first-order kinetic model is limited to describe the experimental kinetic data for the whole biosorption period and can only be applied for preliminary stage of biosorption. Given to the low

correlation coefficient of red and green algae, the pseudo-second-order model was applied to describe the biosorption kinetics.

The  $R^2$  values of pseudo-second-order suggested that this kinetic model was well suited for describing the biosorption of MB onto three different marine algae. The plots of time (min) versus  $q_e$  (mg/g) for the pseudo-second-order model are shown in Fig. 6a–c, and the correlation coefficients  $R^2$  are listed in Table 3. Three distinguished features of this model are: (1) pseudo-second-order model is based on the adsorption capacity, (2) is well for the complete data range of contact time and (3) is in agreement with chemisorption being the rate-limiting step. The results prove that the pseudo-second-order model represents the biosorption kinetics of MB on brown, red and green algae and chemisorption might be the rate-limiting step that controlled the biosorption process.

Four main steps are considered in mass transfer of dye molecules onto the biosorbents: (1) bulk diffusion (transfer from bulk solution to the surface of the biosorbent), (2) film diffusion (transfer through the boundary layer to the biosorbent surface), (3) intra-particle diffusion (transfer from the surface to the interior pores of the particle), (4) chemical reaction via ion-exchange, complexation, chelation; the adsorption of dye at an active site on the biosorbent surface (Kismir and Aroguz 2011).

The intra-particle diffusion model or pore-diffusion mechanism (presented by Eq. 8) and Fig. 6d depicts the linear plot of  $q_t$  versus  $t^{1/2}$ . If intra-particle diffusion occurs then this plot should be a straight line that passes through the origin, when intercept  $C$  equals to zero. The intercept,  $C$  is a constant which reflects information about the thickness effect; i.e., the larger the intercept, the greater the boundary layer effect. As can be seen from Table 3, the value of  $C$  for brown alga is more than twice than the other ones. It proves that the influence of boundary layer affect can be expected for the brown algae rather than red and green algae. The lower correlation coefficients for the intra-particle diffusion model rather than the pseudo-second-order model shows that the process does not obey the intra-particle diffusion model solely.

## 4 Conclusions

The present study examined the biosorption of MB by marine macroalgae. The results suggest that algal biomasses can be effectively used as non-conventional biosorbent for the removal of basic dyes from aqueous solution. The biosorption capacities were mainly influenced by solution pH and optimum pH was found to be  $> 5$  for MB removal by algae. The equilibrium data indicated that the Langmuir model provided the best

correlation of the experimental data for three different marine macroalgae in the concentration range investigated in this study. The results show that the biosorption process was very fast in the first 30 min, and a contact time of 90 min was considered as optimum to achieve a state of equilibrium. Among tested isotherm and kinetic models, Langmuir and pseudo-second-order were found to fit well with the experimental data. The calculated thermodynamic parameters showed the feasibility, endothermic and spontaneous nature of the dye biosorption. The presence of different functional groups on algae surface was found to play an important role in dye biosorption.

**Acknowledgements** This work was financially supported by the Research Council (Postgraduate Education) of Shiraz University (Grant Number 95GCU1M215785).

## References

- Azin E, Moghimi H (2018) Efficient mycosorption of anionic azo dyes by *Mucor circinelloides*: surface functional groups and removal mechanism study. *J Environ Chem Eng* 6(4):4114–4123
- Coates J (2000) Interpretation of infrared spectra, a practical approach. *Encycl Anal, Chem*
- Coelho GF, Gonçalves AC Jr, Tarley CRT, Casarin J, Nacke H, Francziskowski MA (2014) Removal of metal ions Cd (II), Pb(II), and Cr(III) from water by the cashew nut shell *Anacardium occidentale* L. *Ecol Eng* 73:514–525
- Daneshvar E, Kousha M, Jokar M, Koutahzadeh N, Guibal E (2012a) Acidic dye biosorption onto marine brown macroalgae: isotherms, kinetic and thermodynamic studies. *Chem Eng J* 204:225–234
- Daneshvar E, Kousha M, Sohrabi MS, Khataee A, Converti A (2012b) Biosorption of three acid dyes by the brown macroalga *Stoechospermum marginatum*: isotherm, kinetic and thermodynamic studies. *Chem Eng J* 195:297–306
- Daneshvar E, Vazirzadeh A, Niazi A, Kousha M, Naushad M, Bhatnagar A (2017a) Desorption of Methylene blue dye from brown macroalga: Effects of operating parameters, isotherm study and kinetic modeling. *J Clean Prod* 152:443–453
- Daneshvar E, Vazirzadeh A, Niazi A, Sillanpää M, Bhatnagar A (2017b) A comparative study of methylene blue biosorption using different modified brown, red and green macroalgae—Effect of pretreatment. *Chem Eng J* 307:435–446
- Deniz F (2019) Bioremediation potential of waste biomaterials originating from coastal *Zostera marina* L. meadows for polluted aqueous media with industrial effluents. *Prog Biophys Mol Biol* 145:78–84
- Doğan M, Alkan M, Demirbaş Ö, Özdemir Y, Özmetin C (2006) Adsorption kinetics of maxilon blue GRL onto sepiolite from aqueous solutions. *Chem Eng J* 124:89–101
- Freundlich U (1906) Die adsorption in lusungen. *Zeitschrift fur Phys Chemie* 57:385–470
- Gupta VK, Rastogi A (2008) Equilibrium and kinetic modelling of cadmium (II) biosorption by nonliving algal biomass *Oedogonium* sp. from aqueous phase. *J Hazard Mater* 153:759–766
- Gupta VK, Suhas, Ali I, Saini VK (2004) Removal of rhodamine B, fast green, and methylene blue from wastewater using red mud, an aluminum industry waste. *Ind Eng Chem Res* 43:1740–1747
- He J, Chen JP (2014) A comprehensive review on biosorption of heavy metals by algal biomass: materials, performances,

- chemistry, and modeling simulation tools. *Bioresour Technol* 160:67–78
- Khataee AR, Dehghan G (2011) Optimization of biological treatment of a dye solution by macroalgae *Cladophora* sp. using response surface methodology. *J Taiwan Inst Chem Eng* 42:26–33
- Khataee AR, Vafaei F, Jannatkah M (2013) Biosorption of three textile dyes from contaminated water by filamentous green algal *Spirogyra* sp.: kinetic, isotherm and thermodynamic studies. *Int Biodeterior Biodegrad* 83:33–40
- Kismir Y, Aroguz AZ (2011) Adsorption characteristics of the hazardous dye Brilliant Green on Saklıkent mud. *Chem Eng J* 172:199–206
- Kousha M, Daneshvar E, Esmaeili AR, Zilouei H, Karimi K (2014) Biosorption of toxic acidic dye–Acid Blue 25, by aquatic plants. *Desalin Water Treat* 52:6756–6769
- Kousha M, Tavakoli S, Daneshvar E, Vazirzadeh A, Bhatnagar A (2015) Central composite design optimization of Acid Blue 25 dye biosorption using shrimp shell biomass. *J Mol Liq* 207:266–273
- Langmuir I (1918) The adsorption of gases on plane surfaces of glass, mica and platinum. *J Am Chem Soc* 40:1361–1403
- Lee CK, Low KS, Gan PY (1999) Removal of some organic dyes by acid-treated spent bleaching earth. *Environ Technol* 20:99–104
- Lima HH, Maniezzo RS, Llop ME, Kupfer VL, Arroyo PA, Guilherme MR, Rinaldi AW et al (2019) Synthesis and characterization of pecan nutshell-based adsorbent with high specific area and high methylene blue adsorption capacity. *J Mol Liq* 276:570–576
- Mishra G, Tripathy M (1993) A critical review of the treatments for decolourization of textile effluent. *Colourage*
- Papic S, Koprivanac N, Metes A (2000) Optimizing polymer-induced flocculation process to remove reactive dyes from wastewater. *Environ Technol* 21:97–105
- Smaranda C, Bulgariu D, Gavrilescu M (2009) An investigation of the sorption of Acid Orange 7 from aqueous solution onto soil. *Environ Eng Manag J* 8:1391–1402
- Temkin MI, Pyzhev V (1940) Kinetics of ammonia synthesis on promoted iron catalysts. *Acta physiochim URSS* 12:217–222
- Wang G, Liu Q, Chang M, Jang J, Sui W, Si C, Ni Y (2019) Novel Fe<sub>3</sub>O<sub>4</sub>@ lignosulfonate/phenolic core-shell microspheres for highly efficient removal of cationic dyes from aqueous solution. *Ind Crops Prod* 127:110–118
- Zhang Y, Yang L, Wang YH, Liu AH (2019) MoxPy nanoparticles supported on mesh structural carbon from biomass for rapid selective dyes adsorption. *Talanta* 196:9–17